Lithology and Mineral Resources, Vol. 39, No. 4, 2004, pp. 333–344. Translated from Litologiya i Poleznye Iskopaemye, No. 4, 2004, pp. 387–400.

Uranium Distribution in Ore-Bearing Rocks of the Malinov Deposit: Evidence from Fission Radiography

I. A. Kondrat'eva, I. G. Maksimova, and G. I. Nad"yarnykh

Institute of Geology of Ore Deposits, Petrography, Mineralogy, and Geochemistry, Russian Academy of Sciences, Staromonetnyi per. 35, Moscow, 119017 Russia

Received June 30, 2003

Abstract—Application of f-radiography for the study of ore-bearing rocks of the Malinov uranium deposit revealed the following specific features: (1) occurrence of uranium in both authigenic and terrigenous components; (2) important role of fine–dispersed ("mineral-free") mode of uranium occurrence; and (3) participation of different-aged epigenetic processes in the ore formation. The sequence of ore formation and transformation in this deposit is similar to that in the Semizbai deposit. Therefore, they can be united into a single subtype of Mesozoic infiltration deposits in western Siberia.

INTRODUCTION

The Malinov uranium deposit is located in the southwestern part of the Chulym–Yenisei Depression at the boundary with the Kuznetsk–Alatau fold zone. The uranium mineralization has been recovered by boreholes in Late Jurassic–Early Cretaceous alluvial sediments (Tyazhin Formation and lower part of the Kialin Formation) of the buried river valley that cuts Paleozoic metamorphic rocks of the depression basement. The metamorphic rocks are intruded by small granite and granodiorite bodies (Fig. 1).

Geological structure of the deposit is considered in works of Bazhenov *et al.* (1995), Dolgushin *et al.*, (1995), Rubinov *et al.* (2000), Khaldei *et al.* (2000), and Vinokurov *et al.* (2001). Based on the major conditions of uranium mineralization—ore-bearing structure type (erosional-tectonic basal depression), age (Late Jurassic–Early Cretaceous), composition of host rocks (gray alluvial sediments), and presence of signs of epigenetic oxidation—the Malinov deposit is an analogue of deposits located in the Kurgan–Pavlodar uraniferous belt along the periphery of the West Siberian Plate (Kislyakov and Shchetochkin, 2000).

Based on regularities of ore localization, these deposits are ascribed to a single exogenous-epigenetic (infiltration) type related to ground-stratal oxidation in alluvial gray sediments of river paleovalleys. At the same time, it became evident that ore deposits of this belt can be divided into two groups based on the mineral–geochemical composition of ore-bearing sequences, their facies features related to some difference in ages of the origination and evolution of paleovalleys, and regimes of oxygenated water infiltration governing the morphology of uraniferous mineralization. The difference between these two groups is even more prominent in terms of postore (postinfiltrational) processes as a result of different scenarios of the geological evolution of deposit areas (Kondrat'eva and Nesterov, 1997).

Numerous similarities in geological structure and, especially, postore processes at the Semizbai and Malinov deposits made it possible to unite them into the specific Semizbai subtype and include all deposits of the ore-bearing belt into the Semizbai–Dalmatov type (Kondrat'eva and Nesterova, 2002). Vinokurov *et al.* (2001) proposed an alternative genetic concept for the Malinov deposit and suggested that its mineral–geochemical features were governed by intense endogenous ore-forming processes. Hence, this deposit differs from all known ancient and recent uranium deposits of the paleovalley type.

Study of ore-bearing rocks of the Malinov deposit by f-radiography allowed us to obtain additional data on the distribution of uranium and the sequence of formation and transformation (hereafter, evolution) of uranium mineralization.

Investigations were carried out in the Laboratory of Radiogeology at the Institute of Geology of Ore Deposits, Petrography, Mineralogy, and Geochemistry. The majority of samples were taken by Nesterova during the documentation of borehole cores from the central area of the deposit. The f-radiography was developed in the Department of nuclear–physical methods of elemental analysis of rocks and ores at the All-Russia Institute of Nuclear Geophysics and Geochemistry under the supervision of the Academician of the Russian Academy of Sciences G.N. Flerov (Berzina *et al.*, 1967; Flerov and Berzina, 1979). This method is widely applied for the investigation of uranium deposits (*Metody*…, 1985).

The determination of spatial distribution and concentration of uranium in minerals and rocks by this method is based on the thermal neutron-induced fission of uranium into two fragments. The nuclear fragments

0024-4902/04/3904-0333 © 2004 MAIK "Nauka/Interperiodica"

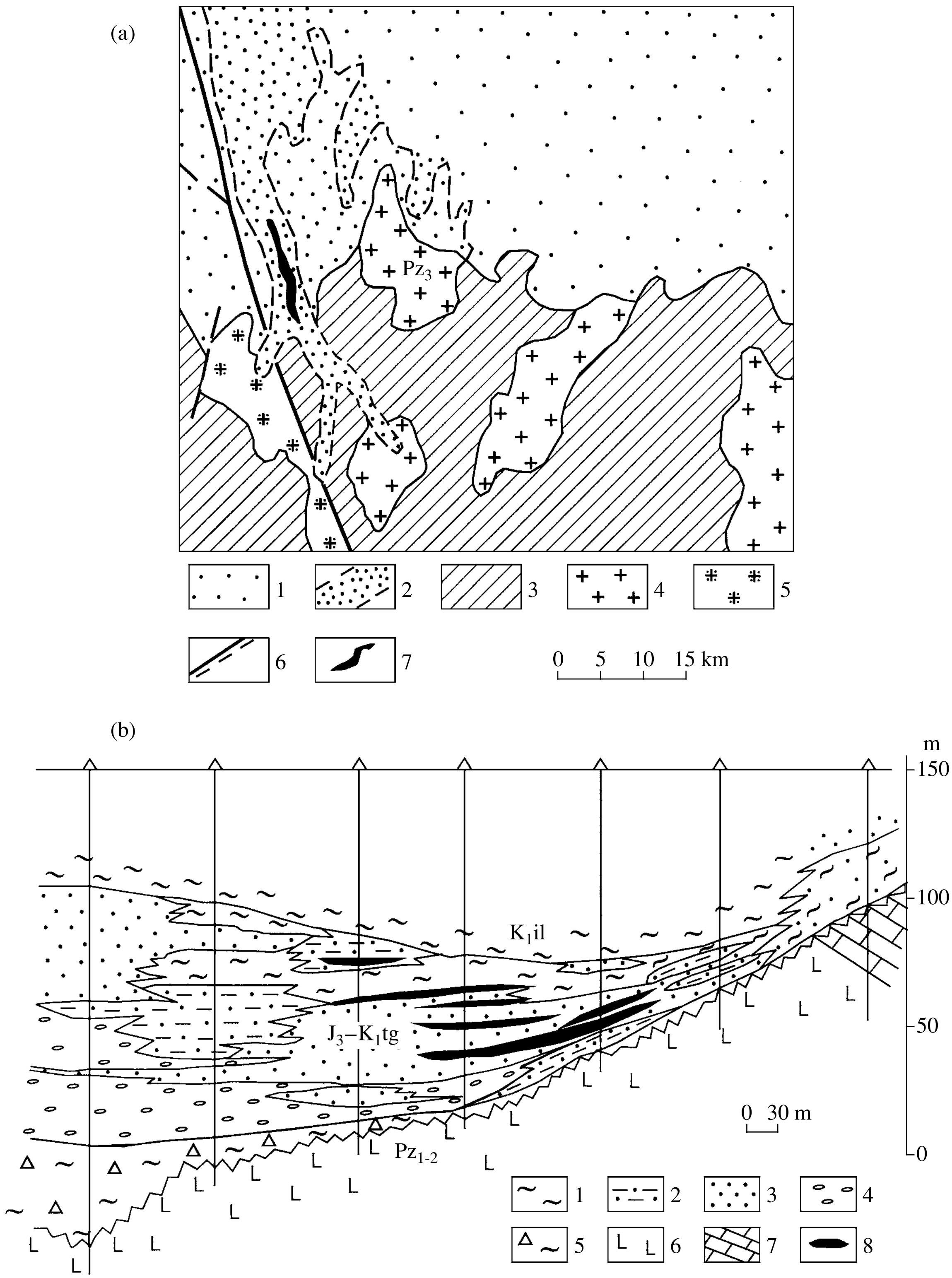

Fig. 1. (a) Schematic geological structure of the southwestern part of the Chulym–Yenisei Depression and (b) geological section of the Malinov Depression. Modified after (Khaldei *et al.*, 2000). (a) (1) sedimentary rocks of the Mesozoic plate complex; (2) Malinov paleovalley; (3) Paleozoic metamorphic complexes; (4) granites; (5) granodiorites; (6) faults; (7) ore-bearing zone. (b) (1) Clays, (2) siltstones and clayey sandstones; (3) sands; (4) gravelstones and conglomerates; (5) weathering crust; (6) volcanic rocks; (7) limestones; (8) ore lodes.

scatter and distort the structure of the host solid body (detector). The fission tracks can be revealed by the chemical etching of detectors. This method has a high sensitivity (up to $n \times 10^{-8}$%) and accuracy of 10–20%. Samples were irradiated by thermal neutrons in the reactor of the Moscow Institute of Engineering Physics. Depending on the U content in samples, the intensity of thermal neutron flux (I) varied from 1×10^{13} to 1×10^{18} n/cm^2.

Polished thin sections of samples were mounted on quartz plates for the investigation. The Mylar coating on the polished thin section was used as detector. The application of quartz plates instead of normal slides significantly decreases the cooling time (induced activity) of thin sections after irradiation.

Study of thin sections and their detectors under microscope (MISAM-212, LOMO Co.) makes it possible to reliably determine the relation of uranium with certain mineral components (or structural elements) of rocks and its distribution pattern. The microscopic documentation of thin sections and detectors was carried out with a digital Kodak MDS-120 camera. Irradiation without "target" (specimen with exactly known U content), which serves as basis for the determination of element content, allowed us to determine the relative U content in different components of the rock based on track distribution and density.

URANIUM DISTRIBUTION IN THE ORE-BEARING AND ORE-HOSTING ROCKS

Study of ore-bearing clastic rocks of the Malinov deposit by f-radiography showed that uranium occurs in both authigenic and terrigenous components.

Uranium in Clastic Grains

The Tyazhin Formation is composed of sandstones, gravelstones, and fine-pebble conglomerates with fragments of various rocks (carbonaceous–siliceous shales, volcanic rocks, and cryptocrystalline siliceous rocks). Petrographically, the clastic material can be ascribed to polymictic graywackes. The f-radiography showed that uranium is often allocated to clastic grains of various compositions. The grains are divided into two groups with respect to uranium distribution. Grains of group 1 are characterized by a uniform uranium distribution (with no traces of gain or loss) over the entire volume. This can be illustrated by rounded fragments of carbonaceous shales (Fig. 2a), as well as grains of cryptocrystalline siliceous rocks and hypergene-altered basalts. It is possible that some grains of group 1 are fragments of primary uraniferous rocks, whereas other grains (e.g., grains of hypergene-altered volcanic rocks) could accumulate uranium during the weathering crust formation. We believe that the uniform distribution of uranium in clastic grains is caused by its introduction in this form into alluvial sediments of the paleovalley and, therefore, can be defined as the presedimentary mode of uranium occurrence.

The possibility of presedimentary uranium concentration is additionally supported by findings of characteristic zonal fragments with a uniform uranium distribution in the central zone and its absence in the contact zone. This type of uranium distribution is seen in the rounded fragment of red mudstone and dacite fragment with iron hydroxide impregnation (Figs. 2b, 2c). Iron hydroxides and uranium are absent in bleached contact zones of the fragments. Bleaching is occasionally developed both along the boundaries of fragments and along the network of cracks.

It is evident that thin bleached rims evenly developed around the fragments could not originate during the transport of clastic material. They presumably formed as a result of the reduction and removal of iron (and associated uranium) in a weakly reducing environment of the buried sediment. In any case, the preservation of uranium in the central zone of fragments indicates the possibility of its introduction into sediments of the paleovalley.

The process of uranium introduction into clastic grains is also intensely developed in the ore-bearing rocks, as indicated by a different type of uranium distribution in clastic grains of group 2. Figure 2d demonstrates a round fragment of dark red mudstone with fine-crystalline pyrite patches corresponding to areas of high track density (HTD). In this case, both pyrite and uranium concentrations demonstrate a distinctly superimposed nature. The process of uranium introduction into clastic grains is widespread in the Malinov deposit (Bazhenov *et al.*, 1995). The intensity of this process is completely governed by rock permeability. For example, uranium concentration associated with pyrite is mainly recorded along fractures in hard siliceous fragments, while the concentration of this element in monolithic grains is confined to their surface. In all cases, uranium is associated with pyrite and its concentration grade suggests the presence of independent mineral phases.

Uranium in Carbonaceous Remains and Clayey Material

Samples with uranium confined to the carbonaceous organic matter are mainly represented by low-permeable rocks (siltstones and fine-grained clayey sandstones). The uranium concentration in fine carbonaceous inclusions is recorded as HTD spots in the detectors (Fig. 3a). The clayey material is also uniform, but its lower track density indicates a relatively lower uranium concentration. Pyrite crystals in such rocks correspond to track-free spots, whereas the clayey component around them is more enriched in uranium than the groundmass.

In these rocks, amorphized biotite flakes, which are transformed into chlorite and smectite, are recorded as uniform HTD spots (Fig. 3b).

In carbonaceous fragments uniform uranium distribution can be supplemented with its concentration on

(a)
(b)
(c)
(d)

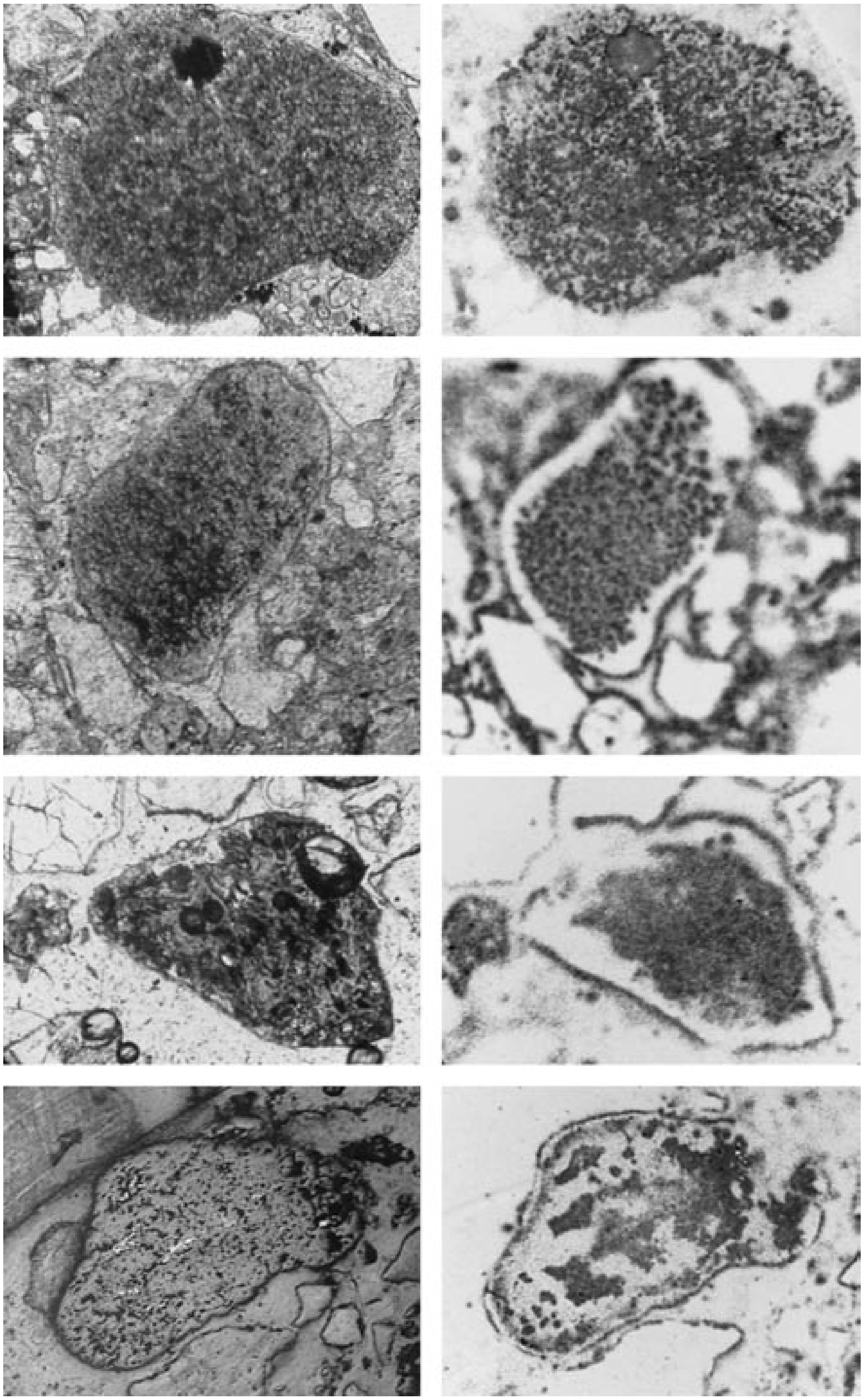

the surface and along the fractures (Fig. 3c). The relation between uranium mineralization in the carbonaceous material and pyrite is illustrated in Fig. 3c. The U-rich carbonaceous fragment is rimmed by large U-free pyrite crystals. The local uranium concentration around pyrite crystals is related to the specimen pollution by abrasive.

The uranium enrichment of carbonaceous material is not universal in the ore-hosting sequence. For example, carbonaceous sediments in the dense clay are completely U-free. Evidently, plants did not accumulate uranium during their vital activity and their remains in impermeable clayey sediments were isolated from groundwaters.

Uranium in Calcite

Sediments of the Tyazhin Formation contain lens-like sandstone interbeds with the epigenetic coarse-crystalline calcite. Since calcite is decomposed and removed during the subsequent transformations of the rock sequence, only its relicts are preserved in the permeable sandy beds. They are well identified in thin sections but invisible during the documentation of borehole cores. The uraniferous calcite has been detected in carbonatized rocks by f-radiography.

Figures 4a and 4b demonstrate photomicrographs of such sandstones recorded by the detectors. Dark fields with a relatively uniform track distribution (UTD) correspond to calcite grains in intergranular space of sandstones. The uranium distribution in calcite can be very intricate. For example, track density in the coarse-crystalline calcite is strongly variable, indicating significant variations of the U content within a single crystalline aggregate (Fig. 4c).

Figure 4d demonstrate a more intricate uranium distribution. One part of the large calcite crystal in the intergranular space is enriched in uranium, whereas another part is nearly uranium-free. However, these two parts are optically similar. The calcite cement in sandstones does not show universal uranium concentration. The cement locally corresponds to track-free areas.

Uranium in Pyritization Zones

Ore-bearing rocks of the Malinov deposit are differently enriched in iron disulfides (mainly pyrite of various modifications and subordinate marcasite). The iron disulfides occur as two epigenetic generations.

The first generation was discussed above during the description of uranium distribution in carbonaceous remains and clayey material.

Iron disulfides of the second generation corrode the coarse-crystalline calcite. Figure 5a shows two pyrite sectors. Calcite cements the sandstone in the first sector. In the second sector, calcite is absent as a result of decarbonatization. The contact zone between these sectors includes pyrite veinlets. Based on f-radiography, calcite is intensely and very unevenly enriched in uranium. The decarbonatization zones include only scarce random tracks. Pyrite crystals correspond to empty spots in the detector. In the ore-bearing sandstones containing only corroded relicts of coarse-crystalline calcite, pyrite crystals are restricted to decarbonatization zones (Fig. 5b). These zones are also characterized by uranium concentration expressed as HTD spots in the detector. Calcite relicts with obvious corrosion traces lack uranium (the relicts are not reflected in the tracks).

Uranium in Chloritization Zones and Iron Hydroxides

The presence of colloform Fe-chlorite in the host rocks of the Malinov deposit has been reported by all investigators. However, its position in epigenetic transformation sequence remains controversial (Khaldei *et al.*, 2000; Kondrat'eva and Nesterova, 2002).

The colloform Fe-chlorite often contains inclusions of powdery iron hydroxide imparting a yellowish color. These aggregates correspond to HTD areas in the detectors (Fig. 5c). However, uranium associates with goethite–chlorite aggregates only within (or at the contact) with uranium lodes, whereas chlorite is more widespread in area and section.

An insignificant uranium enrichment of the powdery iron hydroxide aggregates is also established at the contact of epigenetically oxidized and subsequently reduced clayey rocks.

Uranium in Bitumenization Zones

Droplike inclusions of black lustrous bitumen (asphaltite) have been recorded in sediments of the Malinov Depression by many researchers (Bazhenov *et al.*, 1995; and others).

Fig. 2. Uranium distribution in the clastic grains. Hereinafter: (3–5) photomicrographs of polished thin sections and detectors are given on the left and right sides, respectively. (a, b, c) Transmitted light, (d) reflected light. (a) Round fragment of carbonaceous shale with rare dust of fine-crystalline pyrite and carbonaceous fragment (black). High track density is typical of the whole fragment. Sample C-10-3, magn. $\times 3.7 \times 6$, $I = 5 \times 10^{15}$ n/cm^2. (b) Round fragment of red mudstone with scarce fine crystals of pyrite and marcasite. The contact zone of the fragment is bleached. The central part of the detector is characterized by HTD spots; the light-colored part, by their absence. Sample C-9-4, magn. $\times 3.7 \times 6$, $I = 1 \times 10^{13}$ n/cm^2. (c) Fragment of fluidal microbubble dacite with iron hydroxides and tiny pyrite crystals. Its central part in the detector is characterized by uniform HTD; the peripheral part, by their absence. Sample 36-60, magn. $\times 3.7 \times 6$; $I = 1 \times 10^{13}$ n/cm^2. (d) Fragment of brownish red clayey rock with aggregates of fine pyrite crystals. HTD spots in the detector correspond to the pyritization zone. Sample 36-60, magn. $\times 3.7 \times 6$, $I = 1 \times 10^{13}$ n/cm^2.

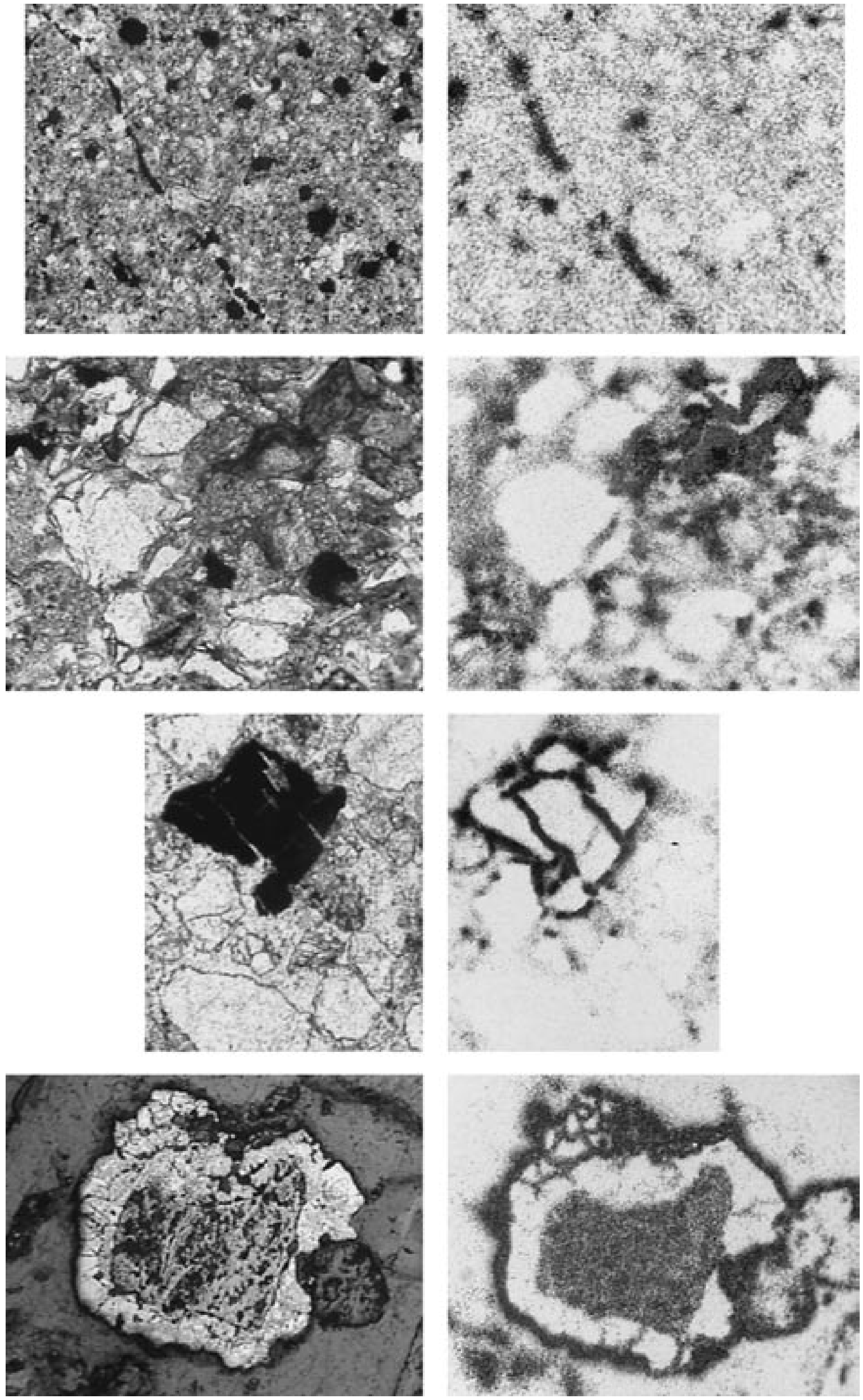

(a)

(b)

(c)

(d)

In the studied sample of dense greenish gray clay, brown bitumen (asphaltite) is restricted to a network of thin branching cracks. The clay matrix along the cracks is saturated with bituminous material (Fig. 5d). Patches of fine pyrite crystals are observed near the bitumen-rich zone. In thin sections, only small asphaltite inclusions are preserved in the cracks. Clayey rocks with brown bitumen are distinctly expressed as HTD spots in the detectors.

DISCUSSION

The track distribution recorded by f-radiography in the detectors makes it possible to estimate both the relative U content in different components of the rocks and its occurrence modes. It has been established that independent uranium phases, which can be identified by optical and electron-microscopic investigations, are characterized by specific track densities and expressed in the detectors as holes produced as a result of the chemical etching of the Mylar coating. However, the high sensitivity of f-radiography also allows one to detect uranium dissemination in other minerals.

Dubinchuk *et al.* (1990) defined such uranium dissemination (mainly, absorbed uranium) as "mineral-free" occurrence mode, which implies the absence of optically observed minerals under any magnification. The f-radiography data indicate an extreme abundance of the mineral-free occurrence mode of uranium in ore-bearing rocks of the deposit.

For example, this element is mainly accumulated in the carbonaceous material and, to a lesser extent, in the clayey material in rocks with organic remains, which lack independent mineral phases of uranium. In addition to the absorbed form, organic compounds of uranium may also be present here.

In the coarse-crystalline calcite, fine-dispersed uranium is randomly distributed and independent mineral phases have not been observed. Calculation of tracks in four calcite domains in Sample C-9-1 (Figs. 4a, 4b) with a relatively uniform uranium distribution yielded the following U contents (%): 0.03, 0.027, 0.038, and 0.026 (average 0.03). More detailed data on the Semizbai deposit indicate that uranium is incorporated in calcite and the U content shows a wide range of variation (average $7 \cdot 10^{-2}$%) (Kondrat'eva *et al.*, 1995).

The association of uranium with the powdery iron hydroxides ("precipitation hydroxides") is consistent with the well-known data on intense uranium sorption by these minerals. This phenomenon is widespread in the Semizbai deposit (Kondrat'eva *et al.*, 1992, 1997; Kislyakov and Shchetochkin, 2000).

Independent uranium minerals are recorded as small holes in the Mylar coating (mainly in cracks and on the surface of fragments) and universally associate with pyrite. According to data presented in (Bazhenov *et al.*, 1995; Khaldei *et al.*, 2000; Vinokurov *et al.*, 2001), ores of the Malinov deposit contain the major coffinite, the subordinate uranium oxides, and the scarce ningyoite. All researchers noted that mineral aggregates are strongly dispersed and confined to iron disulfides.

Thus, ores of the Malinov deposit contain uranium as both fine-dispersed minerals and abundant fine dissemination of the mineral-free phase, which is typical of exogenous-epigenetic uranium deposits. Hence, assessment of the ore potential of such objects requires not only the description of uranium minerals, but also calculations of U budget. The uranium budget in ores has both genetic and applied significance. Therefore, it must be taken into account in underground leaching, which is the most efficient method for the exploitation of such ores.

The multistage evolution of uranium mineralization in the Malinov deposit supported by f-radiography is its second characteristic feature. This implies the contribution of processes of the infiltration stage, which controlled the spatial position of mineralization, as well as the preore and postore stages, which governed all characteristic features of the deposit.

The ore-enclosing sequences contain rock fragments with the characteristic uranium distribution (uniform distribution over the entire grain and local signs of removal), suggesting the possible existence of presedimentary uranium. However, absence of data on the distribution of such fragments in sediments of the paleovalley casts doubt on this assumption. In any case, the input of uranium in rock fragments was not an ore-forming process. This material could serve only as an additional source of uranium during the subsequent ore formation.

Ores confined to low-permeable rocks (siltstones and fine-grained clayey sandstones enriched in plant remains and pyrite) are probably the earliest ones. They

Fig. 3. Uranium distribution in the carbonaceous remains and clayey material. (a, b, c) Transmitted light, (d) reflected light. (a) Clayey siltstone with carbonaceous remains and abundant tiny pyrite crystals. HTD corresponds to carbonaceous fragments; clayey material is characterized by uniform-disseminated track distribution. Sample C-88-1, magn. ×9, $I = 1 \times 10^{14}$ n/cm^2. (b) Fine-grained clayey sandstone with abundant intercalated carbonaceous remains (absent in the studied thin section) and scarce pyrite. Clayey cement in the detector is expressed as uniform but low track density; HTD spot corresponds to amorphized chloritized fragment of biotite. Sample C-141-2, magn. ×9, $I = 1 \times 10^{13}$ n/cm^2. (c) Carbonaceous fragment in the medium-grained sandstone. HTD in the detector corresponds to the outer contour and cracks in the carbonaceous fragment. Sample C-2-2, magn. ×3.7 × 4, $I = 1 \times 10^{13}$ n/cm^2. (d) Carbonaceous fragment surrounded by coarse-crystalline pyrite. Coal in the detector is characterized by uniform HTD; pyrite, by their nearly complete absence. Sample C-36-60, magn. ×9, $I = 1 \times 10^{13}$ n/cm^2.

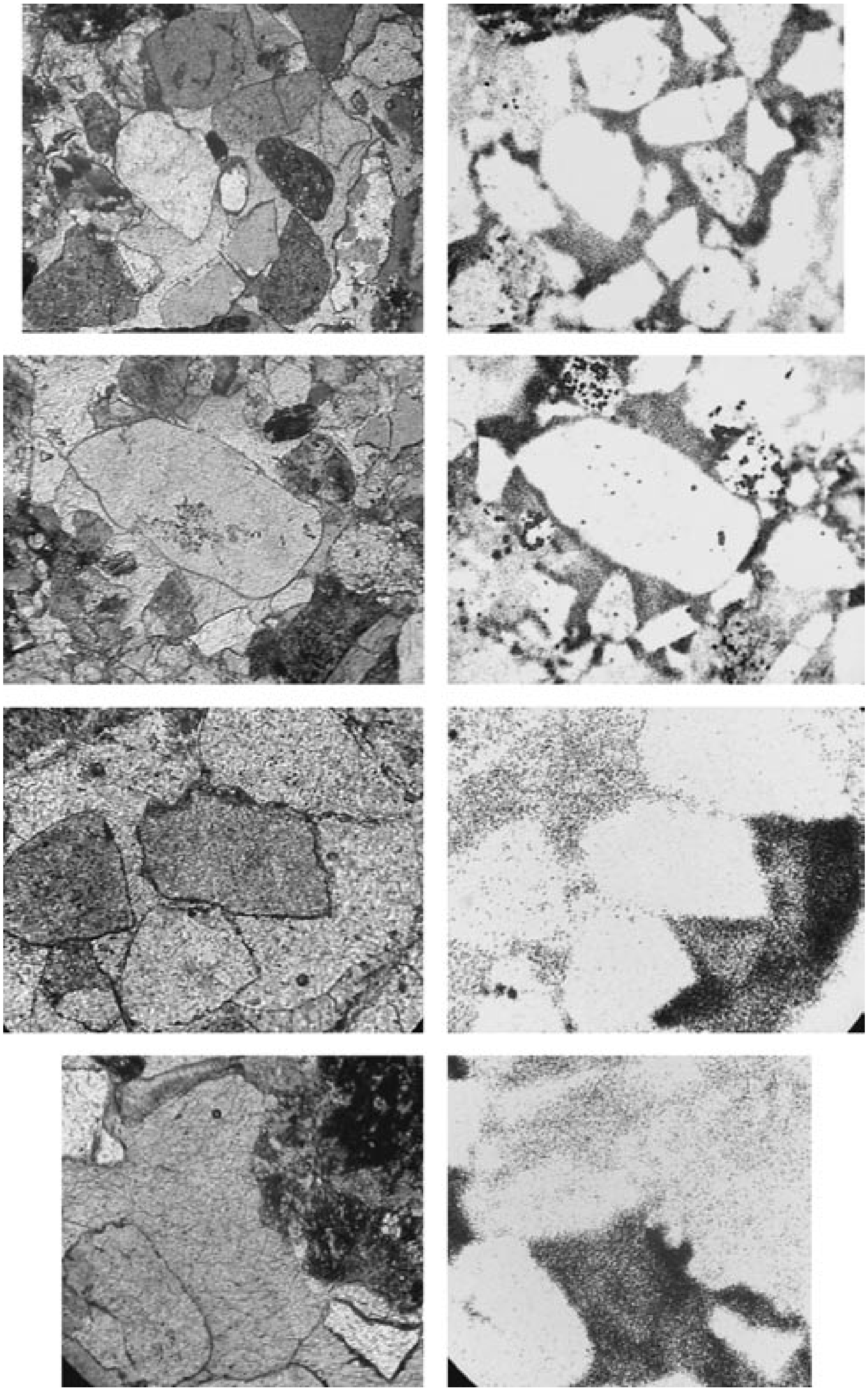

(a)

(b)

(c)

(d)

are characterized by uranium concentration in carbonaceous remains and uranium dissemination in the clayey material. Taking into consideration signs of oxidation in the low-permeable gray rocks at the contact with the permeable sandy horizons and their intense epigenetic alteration, one can assume that uranium mineralization produced by oxygenated infiltration waters is preserved precisely in the relatively less permeable beds. In this case, the carbonaceous material serves as the main factor responsible for the creation of reducing uranium barrier. The presence of pyrite dissemination can also be related to infiltrational processes. It is known that pyritization zone produced by biochemical oxidation of the organic matter is an essential member of the oxidizing ore-controlling zoning in rocks containing carbonaceous plant remains (*Gidrogennye…*, 1980).

As was shown above, the ore-bearing sequence of the Malinov deposit contains lenslike sandstone interbeds with coarse-crystalline calcite cement, in which f-radiography discovered the uraniferous calcite. It was also established that the calcite cement not universally contains uranium and its distribution is very intricate (Figs. 4c, 4d). According to Vinokurov *et al.* (2001), the calcite formation temperature varies from 120 to 230°C. These values correspond to low- and moderate-temperature hydrothermal solutions.

Similar but larger-scale carbonatization is developed in the Semizbai deposit. Study of carbonatization at this extensively drilled object made it possible to estimate conditions of the uraniferous calcite formation (Kondrat'eva *et al.*, 1992, 1995; Kondrat'eva and Nesterova, 1997). It was established that the coarse-crystalline calcite was produced as a result of the penetration of low-temperature CO_2-rich hydrothermal solutions from the granite basement of the depression into sedimentary cover along fracture zones. The solutions did not contain uranium, but they promoted the partial dissolution of the older infiltrational ores and redeposition of uranium and calcite during the carbonatization.

It is possible that similar conditions also existed in the Malinov deposit. The presence of uraniferous calcite indicates that the ore-bearing rocks were enriched in uranium and served as its source during the carbonatization. Evidently, the uranium concentrations were related to infiltrational processes in alluvial deposits of the paleovalley, since traces of other ore-forming processes predating the carbonatization are absent (Kondrat'eva and Nesterova, 2002).

Like the counterpart in the Semizbai deposit, the coarse-crystalline calcite cement in sandstones of the Malinov deposit serves as a reliable marker between mineral assemblages formed before and after the carbonatization.

Distinct corrosion interrelations with calcite indicate that Fe-chlorite and late iron disulfides also formed at postcarbonate stages in the Malinov deposit.

According to Khaldei *et al.* (2000), chloritization of productive rocks is typical of the entire drilled section of the Malinov paleovalley and the largest aureoles are developed in sandy rocks. The intensity of chloritization increases above tectonic dislocations in the crystalline basement, which also contains the chlorite mineralization. Based on X-ray analysis data, colloform chlorite is represented by the Fe-rich variety (leptochlorite) and locally devitrified. Chloritization is also superimposed on the uraniferous rocks, as suggested by the development of green colloform chlorite segregations around clastic grains and lamellar chlorite grains after the smectite cement. However, evidence of uranium deposition or redeposition related to chloritization has not been found.

It is distinctly seen in thin sections that the coarse-crystalline calcite in carbonatized sandstones is corroded by the colloform chlorite. Intensely chloritized sandstones only contain small calcite relicts, suggesting the decomposition and removal of this mineral (Kondrat'eva and Nesterova, 2002).

The colloform chlorite often associates with the brown-yellow powdery iron hydroxides concentrated around relicts of plant remains at the contact of beds. The microscopic inclusions of iron hydroxides occasionally impart a brownish tint to the colloform chlorite. The f-radiography discovered uranium in such goethite–chlorite aggregates (Fig. 5c). This is consistent with high U contents ($n \times 10^{-3}$–10^{-2}%) in chloritized sandstones near the contact with gray ore-bearing rocks.

The chlorite mineralization of the Malinov deposit resembles the second mineral assemblage of the post-ore hydrothermal stage at the Semizbai deposit represented by variable-composition colloform aggregates

Fig. 4. Uranium distribution in calcite. (a, b) Crossed nicols, (c) plane-polarized light. (a) Medium-grained sandstone with coarse-crystalline calcite cement. In the detectors, calcite is characterized by uniform HTD; some fragments, by scarce HTD spots. Sample C-9-1, magn. ×3.7, I = 1 ×10^{14}n/cm^2. (b) Varigrained sandstone with calcite cement. Calcite in the detector is characterized by uniform track distribution; some clastic grains, by spotty distribution. Sample C-9-1, magn. ×3.7, I = 1 × 10^{14} n/cm^2. (c) Coarse-grained sandstone with poikilitic calcite cement. Calcite crystals yield spots with tracks ranging from high-density (black field) to uniform-disseminated types. The track concentration (U content) shows does not affect optical properties of calcite. Sample C-10-1, magn. ×9, I = 1 × 10^{14} n/cm^2. (d) Coarse-grained calcite in the intergranular space of sandstone. Calcite field in the detector is characterized by heterogeneous track distribution: one part yields fairly high-density (up to continuous) distribution, while the disseminated part yields small HTD spots. Difference in the U content does not affect optical properties of calcite. Sample C-9-1, magn. ×3.7 × 6, I = 1 × 10^{14} n/cm^2.

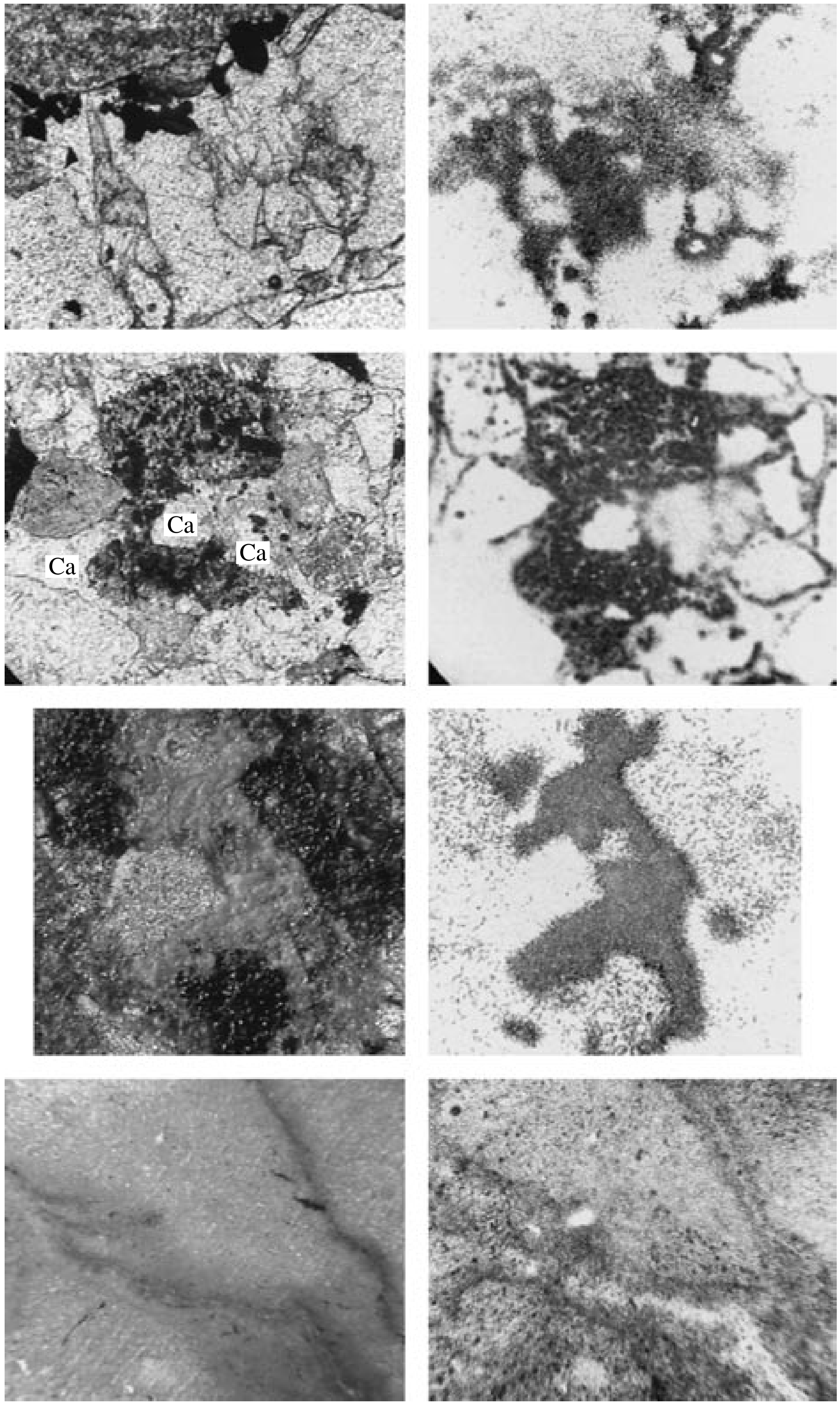

(a)

(b)

(c)

(d)

with alternating concentric zones of Fe-chlorite, nontronite, and goethite. This assemblage distinctly corrodes the coarse-crystalline calcite and forms thin veinlets in calcite veins in the granite basement of the depression. Its formation is related to the penetration of weakly acid, Fe-rich H_2S-free (gleyey) waters from the basement into the sedimentary cover (Kondrat'eva *et al.*, 1992; Kondrat'eva and Nesterova, 1997).

We believe that the coexistence of powdery iron hydroxides and colloform chlorite in the Malinov deposit is caused by the precipitation of hydroxides from the same Fe-rich gleyey solutions, which generated the chlorite, rather than the oxidation of this mineral. Such hydroxides do not indicate oxidizing (infiltration) processes. It is evident that sandy rocks of the Malinov deposit were chloritized after the infiltrational ore formation and carbonatization. The input of uranium is not related to this process, but the penetration of Fe-rich solutions from the basement could locally redistribute uranium near the older ore lodes.

In ore-bearing rocks of the Malinov deposit, iron disulfides are abundant. Moreover, one can suppose that they are polychronous formations. Issue of the presence of diagenetic sulfides proposed by Khaldei *et al.* cannot be solved on the basis of the available data.

We can recognize two pyrite generations ascribed to two different epigenetic stages. The first epigenetic pyrite is observed as dissemination in the clayey material of low-permeable uraniferous rocks with carbonaceous plant remains (Fig. 3a). As mentioned above, such pyrite grains are confined to the low-permeable beds with frequent signs of oxidation (limonitization) at the contact with aquiferous horizons, suggesting their affiliation to the infiltration stage.

The position of the second epigenetic iron disulfide is in the mineralization sequence is defined by its interrelation with carbonatized rocks. Figure 5a shows that the contact between the coarse-crystalline calcite and decarbonatization (calcite removal) zone is filled with pyrite crystals that corrode the calcite grains. The postcarbonate origin of pyrite is evident in this case. Pyrite occurs in decarbonatization zones in the sandstones with calcite relicts (Fig. 5b). This generation presumably includes pyrite overgrowths on the uraniferous carbonaceous fragment with the fine-dispersed uranium mineralization related to infiltrational processes (Fig. 3d). It is possible that the fine-crystalline pyrite in the clastic grains also belong to this generation. As shown above, uranium can associate with the late pyrite generation (Fig. 5b), but this phenomenon is intricate and not universal.

The uranium concentration in the late pyrite generation is restricted to ore-bearing rocks of the paleovalley, indicating that uranium was derived from the older uranium deposits in the same rocks. The import of uranium is highly improbable under these conditions. It is worth mentioning that the Semizbai deposit includes a late pyrite generation that replaces the carbonatized rocks and corrodes the coarse-crystalline calcite. Under certain conditions, uranium associates with this pyrite generation (Kondrat'eva *et al.*, 1992; Kondrat'eva and Nesterova, 1997).

When investigating the origin of late iron disulfides, one should take into account the presence of bitumens in rocks of the Malinov depression. Indeed, scarce droplike bitumen inclusions have been noted in the sandy beds by all researchers. The fact of bitumen penetration into the clayey roof of the sandy beds along fissures should also be taken into account (Fig. 5d). In the latter case, we evidently observe relicts of a liquid bituminous matter migrating along the sandy bed adjoining the clayey rocks.

It is known that bitumen in aquifers underwent the biochemical oxidation by sulfates of groundwaters, resulting in the generation of CO_2 and H_2S. Sulfides formed in this process replace bitumens in aquiferous horizons, whereas their relicts in low-permeable rocks can be preserved. This trend has been established in infiltrational uranium deposits in the oil-and-gas-bearing rocks, such as carbonate rocks of the northern Fergana region, Cretaceous terrigenous rocks of the southern Kyzylkum region, and others (Kholodov *et al.*, 1961; *Gidrogennye…*, 1980; Pen'kov *et al.*, 1982; and others). This suggests that H_2S of late sulfides in the Malinov deposit was derived from the biochemical oxidation of bitumens delivered from the West Siberian oil-and-gas province to sediments of the paleovalley. It should be noted that Upper Jurassic–Early Cretaceous ore-hosting sediments of the depression are stratigraphic counterparts of the Bazhenov Formation, one of the main productive formations in this province.

Fig. 5. Uranium distribution in zones of propylitization, chloritization, and bitumenization. (a, b, c) Transmitted light, (d) oblique light. (a) Coarse-crystalline calcite in the intergranular space of sandstone and decarbonatized zone (upper left corner) with pyrite aggregates along their contact. Calcite is characterized by intense but uneven track distribution in the detector. Sample C-9-1, magn. $\times 9$, $I = 1 \times 10^{14}$ n/cm^2. (b) Sandstone with calcite relict. Dark areas are decarbonatized zones with pyrite accumulations. In the detectors, they correspond to HTD spots. Calcite is not recorded by tracks in the detector. Sample C-88-2, magn. $\times 3.7 \times 6$, $I = 1 \times 10^{13}$ n/cm^2. (c) Colloform brownish green chlorite in the intergranular space of sandstone. In the detector, it is expressed as UTD areas. Sample 36-13, magn. $\times 9 \times 4$, $I = 1 \times 10^{13}$n/cm^2. (d) Dense lamellar clay with a thin branching crack rimmed by brown bituminous material with scarce inclusions of black lustrous bitumen. HTD corresponds to areas of bitumen-rich clays. Sample C-2-1, magn. $\times 2.5$, $I = 1 \times 10^{14}$ n/cm^2.

CONCLUSIONS

Application of f-radiography for the study of ore-bearing rocks of the Malinov deposit made it possible to reveal some specific features of uranium mineralization in this area.

In addition to fine-dispersed uranium minerals, the disseminated (mineral-free) form is also present in ore-bearing rocks of this deposit. The mineral-free uranium associates with the carbonaceous material, clay minerals, calcite, and iron hydroxides. The presence of disseminated uranium indicates that the investigation of such objects must take into account both mineral and other modes of its occurrence. This is important for not only genetic conclusions, but also the accomplishment of underground leaching of ores.

Ores of the Malinov deposit are products of different stages of the evolution of ore-bearing rocks. Major regularities of ore localization in alluvial sediments of the paleovalley and direct indications of oxidizing transformations support the concept of infiltrational genesis of the Malinov deposit proposed by many researchers (Bazhenov *et al.*, 1995; Dolgushin *et al.*, 1995; Rubinov *et al.*, 2000; Khaldei *et al.*, 2000; Kondrat'eva and Nesterova, 2002). According to this concept, uranium ores of this deposit mainly formed at the infiltration stage, whereas the preore and postore processes are subordinate.

The sequential and compositional features of epigenetic processes related to the evolution of ores of the Malinov deposit are similar to those in the Semizbai deposit. Geological settings of these deposits are also similar. Therefore, one can include them into the Semizbai subtype of Mesozoic infiltrational deposits in western Siberia.

ACKNOWLEDGMENTS

We thank I. M. Rubinov, chief geologist of the Berezovgeologiya Association, for several samples placed at our disposal.

REFERENCES

Bazhenov, M.I., Mashkovtsev, G.A., Rasulova, S.D., Tarkhanova, G.A., and Khaldei, A.E., Lithogeochemical Constraints of the Localization of the Uranium–Polymetal Mineralization in the Malinov Deposit, *Materialy po geologii urana, redkikh i redkozemel'nykh metallov* (Materials Related to the Geology of Uranium, Rare, and Rare Earth Metals), Moscow: Vseross. Inst. Mineral. Syr'ya, 1995, pp. 46–61.

Berzina, I.G., Berman, I.B., Gurvich, M.Yu., Flerov, G.N., and Shimelevich, Yu.S., Determination of Uranium Concentration and Distribution in Minerals and Rocks, *Atomn. Energ.*, 1967, vol. 23, no. 6.

Dolgushin, L.S., Bazhenov, M.I., Rubinov, I.M., and Zadorin, L., The Malinov Uranium Deposit, *Otechestven. Geol.*, 1995, no. 9, pp. 39–42.

Dubinchuk, V.T., Kochenov, A.V., Ruzhitskii, V.V., and Meshchankina, V.I., Exogenic-Epigenetic Uranium Mineralization in Sedimentary Rocks Based on Electronic Microscopy Data, *Litol. Polezn. Iskop.*, 1990, vol. 25, no. 3, pp. 65–72.

Flerov, G.N. and Berzina, I.G., *Radiografiya mineralov gornykh porod i rud* (Radiography of Minerals in Rocks and Ores), Moscow: Atomizdat, 1979.

Gidrogennye mestorozhdeniya urana. Osnovy teorii obrazovaniya (Hydrogenic Uranium Deposits: Fundamentals of the Formation Theory), Moscow: Atomizdat, 1980.

Khaldei, A.E., Tarkhanova, G.A., Rasulova, S.D., Kochenov, A.V., Dubinchuk, V.T., and Bazhenov, M.I., Sequence of Epigenetic Transformations and Uranium Mineralization in the Malinov Deposit, *Materialy po geologii mestorozhdenii urana, redkikh i redkozemel'nykh metallov* (Materials Related to the Geology of Uranium, Rare, and Rare Earth Metals), Moscow: Vseross. Inst. Miner. Syr'ya, 2000, pp. 172–192.

Kholodov, V.N., Lisitsin, A.K., Komarova, G.V., and Kondrat'eva, I.A., Epigenetic Zoning of Uranium Mineralization in Oil-Bearing Carbonate Rocks, *Izv. Akad. Nauk SSSR, Ser. Geol.*, 1961, no. 11, pp. 50–63.

Kislyakov, Ya.M. and Shchetochkin, V.N., *Gidrogennoe rudoobrazovanie* (Hydrogenic Ore Formation), Moscow: Geoinformmark, 2000.

Kondrat'eva, I.A. and Nesterova, M.V., Lithogeochemical Features of Uranium Deposits in Mesozoic River Paleovalleys, *Litol. Polezn. Iskop.*, 1997, vol. 32, no. 6, pp. 577–594 [Lithol. Miner. Resour. (Engl. Transl.), 1997, vol. 32, no. 6, pp. 505–520].

Kondrat'eva, I.A. and Nesterova, M.V., Infiltrational Uranium Deposits in Mesozoic River Paleovalleys in Western Siberia, *Uran na rubezhe vekov: prirodnye resursy, proizvodstvo, potreblenie* (Uranium at the Boundary of Centuries: Natural Resources, Production, and Consumption), Moscow: Vseross. Inst. Miner. Syr'ya, 2002, pp. 144–159.

Kondrat'eva, I.A., Bobrova, L.L., and Nesterova, M.V., Role of Postore Processes in the Transformation of an Ancient Infiltrational Uranium Deposit, *Litol. Polezn. Iskop.*, 1992, vol. 27, no. 1, pp. 70–90.

Kondrat'eva, I.A., Maksimova, I.G., and Doinikova, O.I., Conditions of the Formation of U-Bearing Calcite in Ore-Enclosing Rocks of the Semizbai Deposit (Kazakhstan), *Geol. Rudn. Mestorozhd.*, 1995, vol. 37, no. 1, pp. 89–96.

Metody izucheniya uranovykh mestorozhdenii v osadochnykh i metamorficheskikh tolshchakh (Methods for the Study of Uranium Deposits in Sedimentary and Metamorphic Sequences), Moscow: Nedra, 1985.

Pen'kov, V.F., Kondrat'eva, I.A., Shmariovich, E.M., *et al.*, Uraniferous Bitumens in a Deposit Related to Stratal Oxidation Zones, *Litol. Polezn. Iskop.*, 1982, no. 2, pp. 70–84.

Rubinov, I.M., Bazhenov, M.I., Udovik, V.V., and Brednikhin, I.F., The Malinov Uranium Deposit in the West Siberian Uranium Ore Belt, *Uran na rubezhe vekov: prirodnye resursy, proizvodstvo, potreblenie* (Uranium at the Boundary of Centuries: Natural Resources, Production, and Consumption), Moscow: Vseross. Inst. Miner. Syr'ya, 2000, pp. 60–61.

Vinokurov, S.F., Doinikova, O.A., Krylova, T.L., Men'shikov, V.V., Nesterova, M.V., Ryzhov, B.I., and Sysoev, A.N., Lithogeochemical and Mineralogical Features of the Malinov Uranium Deposit (Russia), *Geol. Rudn. Mestorozhd.*, 2001, vol. 43, no. 5, pp. 414–429 [Geol. Ore Deposits (Engl. Transl.), 2001, vol. 43, no. 5, pp. 371–385].